Faraday Discussions

Cite this: *Faraday Discuss.*, 2025, **260**, 377

ROYAL SOCIETY OF CHEMISTRY

PAPER

View Article Online
View Journal | View Issue

Near-infrared responsive three-component supramolecular hydrogels of peptide, agarose and upconversion nanoparticles†

Ivo Rosenbusch, Dominik Mählmann and Bart Jan Ravoo *

Received 20th December 2024, Accepted 30th January 2025
DOI: 10.1039/d4fd00203b

Self-assembled, low molecular weight hydrogels are of particular interest for the development of responsive materials because they exhibit tunable viscoelasticity, high water content, and shear-thinning behavior, which make them suitable for various applications as biomimetic materials. Moreover, such hydrogels are quite easy to prepare. Here, a three-component gel is prepared by adding the peptide AAP-FGDS to an agarose polymer network. The photoresponsive peptide hydrogel exhibits excellent reversible properties. The photoisomerization of the peptide is enabled by lanthanide-doped upconversion nanoparticles (UCNP) added as a third component in the gel. UCNP can convert excitation in the near infrared (NIR) range into emission of higher energy through the process of upconversion. Irradiation with an NIR laser dissolves the self-assembled three-dimensional network structure of the peptide, resulting in a softer hydrogel. The three-component supramolecular gel can potentially be used for *in vivo* applications considering the fact that (unlike harmful UV light) NIR light can penetrate deeply into tissue.

Introduction

Hydrogels based on self-assembling peptides have garnered significant interest due to their biocompatibility, structural versatility, and ability to form well-defined supramolecular networks under mild conditions. These peptide-based hydrogels can be precisely tailored to exhibit specific mechanical properties and response to external stimuli, such as pH, temperature, and light. Many researchers have demonstrated the potential of peptide-based hydrogels as responsive materials, capable of adapting their structure and function in response to their environment. Their studies further highlight how these systems

Center for Soft Nanoscience and Organic Chemistry Institute, University of Münster, 48149 Münster, Germany. E-mail: b.j.ravoo@uni-muenster.de

† Electronic supplementary information (ESI) available: Analytical data, spectra and additional experimental details. See DOI: **https://doi.org/10.1039/d4fd00203b**

combine molecular programmability with biological functionality, making them ideal candidates for applications in regenerative medicine, tissue engineering, and controlled drug delivery.[1–3]

Peptide-based hydrogels have emerged as versatile materials due to their ability to self-assemble into well-defined supramolecular networks through non-covalent interactions. The primary driving forces for hydrogel formation include the hydrophobic effect, π–π stacking interactions, hydrogen bonding, and van der Waals forces, all of which contribute to the stability and tunability of these materials. In particular, the hydrophobic residues within peptides minimize unfavorable interactions with water, while π–π stacking interactions among aromatic residues reinforce the structural integrity of the gel network. These interactions are further complemented by hydrogen bonding along the peptide backbone, providing dynamic reversibility and adaptability in response to environmental stimuli such as pH, temperature, and light.[4–6]

In the context of photoresponsive hydrogels, the integration of molecular photoswitches such as arylazopyrazole (AAP) introduces a unique dynamic component, enabling controlled phase transformations *via* external light stimuli. Upon UV irradiation, the AAP moiety undergoes photoisomerization from the *trans* (*E*-isomer) to *cis* (*Z*-isomer) configuration, disrupting π–π stacking and hydrophobic interactions within the peptide network. This transition results in a gel-to-sol transformation, as observed in the AAP-FGDS system. Reversion to the *trans* isomer through visible light exposure restores these interactions, reassembling the gel network and recovering its mechanical properties.[7]

Incorporating lanthanide-doped upconversion nanoparticles (UCNP) into these systems allows precise excitation of the AAP moiety with biocompatible near-infrared (NIR) light, eliminating the need for harmful UV irradiation. The UCNP-mediated energy transfer enables localized and efficient photoisomerization, offering a high degree of control over gel mechanics and phase behavior. Additionally, agarose is often introduced into peptide-based hydrogels to enhance mechanical stability, reduce the concentration of peptide gelators required, and support the formation of a dual network architecture.

In this respect, a study by Yan *et al.*[8] highlights the potential of UCNP for on-demand biomolecule release from hydrogels. In that case, a polymer-based hydrogel was used to encapsulate UCNP and biomolecules, where the gel-to-sol transition is triggered by NIR light. The hydrogel consisted of a cross-linked polymer network of polyethylene glycol (PEG), which provides mechanical stability and at the same time enables the absorption of UCNP. Upon irradiation with NIR light, the UCNP emit higher-energy photons through upconversion, which locally disrupt the polymer network, resulting in a controlled release of the encapsulated biomacromolecules. This release mechanism ensures that the bioactivity of proteins or enzymes remains intact, making the system suitable for therapeutic applications. Several other studies have shown that UCNP can be integrated into both polymer- and peptide-based hydrogels to achieve light-sensitive functions. For example, polymer-based hydrogels have been extensively studied for controlled drug delivery and photodynamic therapy as they effectively encapsulate UCNP while maintaining their structural integrity. In contrast, peptide-based hydrogels, which assemble into supramolecular networks through non-covalent interactions, have also been explored as biocompatible platforms for UCNP applications. Overall, these highlight the versatility and wide-

ranging applicability of UCNP-loaded hydrogels in areas such as tissue engineering, drug delivery and smart materials.[1,9–11]

Building on this foundation, various groups have explored the versatility of peptide-based hydrogels by integrating them with magnetic nanoparticles, polymers, or UCNP to achieve unique responsive properties. Notably, Nowak *et al.* reported the photoresponsive dual network hydrogels by combining the peptide gelator AAP-FGDS with a covalent agarose network. This hydrogel displayed phototunable mechanical properties and remarkable shape memory behavior. Upon UV light irradiation, the self-assembled peptide network disaggregated, softening the hydrogel while retaining its structural integrity. Irradiation with visible light enabled the reassembly of the peptide network, allowing programmed shape changes and recovery of the original structure through mechanical deformation.[7]

In a subsequent study, our team demonstrated the incorporation of magnetite nanoparticles into a peptide-based hydrogel formed by the gelator Nap-GFYE. The nanoparticles acted as physical crosslinkers, enhancing the gel's mechanical properties while imparting magnetic susceptibility. Under a weak magnetic field, the material exhibited a gel-to-sol transition and enabled on-demand release of encapsulated cargo, such as fluorescent dyes, into the supernatant. Expanding on this, we introduced a dual-responsive hydrogel that reacts to both magnetic fields and light. This system was based on the co-assembly of the AAP-modified peptide Nap-GFFYS with cyclodextrin vesicles containing cobalt ferrite nanoparticles. Under a magnetic field, the gel exhibited an increase in storage modulus, enabling macroscopic manipulation such as bending of gel rods with a weak permanent magnet. Simultaneously, the host–guest interactions between the AAP-peptide and the cyclodextrin vesicles were reversibly disrupted upon UV or visible light irradiation, providing dynamic control over the gel's mechanical stiffness.[12,13]

Complementing these efforts, Möller *et al.* introduced the first example of AAP switching in the presence of UCNP. In this study, cyclodextrin-coated UCNP acted as hosts for azobenzene and AAP guests. The isomerization of these photoresponsive guests was achieved through irradiation with a 980 nm NIR laser, showcasing the potential of UCNP for precise photocontrol in biocompatible systems.[14]

Together, these studies highlight the significant advancements in peptide-based hydrogels, demonstrating their ability to integrate nanoparticles and polymers for achieving responsive behavior to external stimuli such as magnetic fields, UV/visible light, and NIR light. This work presents a three-component hydrogel that incorporates a dual network architecture to leverage both mechanical robustness and dynamic response. These multifunctional hydrogels showcase tremendous potential for applications in drug delivery, soft robotics, and smart material design. Collectively, these advancements reflect a broader trend toward developing versatile hydrogel systems for therapeutic and diagnostic applications, paving the way for next-generation smart materials.[15–20]

The three-component hydrogel reported here integrates a photoresponsive low molecular weight gelator (LMWG) network, AAP-FGDS, with a non-responsive polymeric network of agarose to enhance the mechanical and colloidal stability of the hydrogel.[21,22] In addition, lanthanide-doped UCNP enable the modulation of the gel stiffness by NIR irradiation (Fig. 1). In this approach, UCNP are

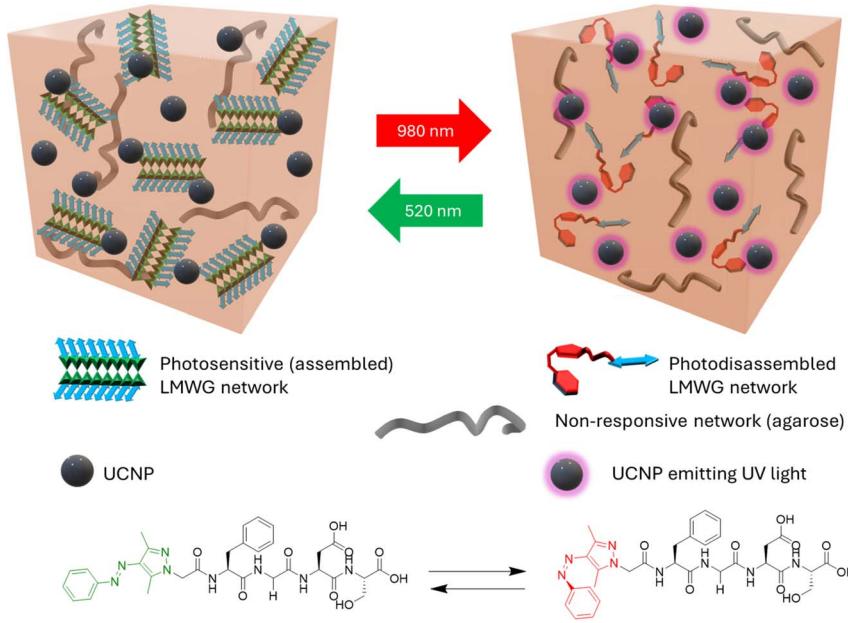

Fig. 1 Schematic illustration of the NIR responsive three component hydrogel. On the left, the light-responsive low molecular weight gelator (LMWG) network is shown in its assembled form, with UCNP embedded in the network and agarose providing mechanical and colloidal stabilization. Upon irradiation with NIR light at 980 nm (red arrow), photodissociation of the peptide network occurs, leading to gel weakening (right side). When exposed to visible light at 520 nm (green arrow), the gel returns to its original state, triggering the reassembly of the LMWG network. The reversible photoisomerization of the AAP-FGDS peptide, which drives this process, is shown below.

embedded in a hydrogel. UCNP convert NIR light (980 nm) into higher-energy photons, enabling photoisomerization of the LMWG component without the need for potentially harmful UV light. Upon NIR irradiation, the UCNP mediate the photoisomerization of the AAP-FGDS gelator, resulting in reversible dissociation of the LMWG network. This process offers precise control over the hydrogel properties, allowing for gel-to-sol transitions triggered by biocompatible NIR light. The integration of UCNP enhances the applicability of this system for *in vivo* applications, including drug delivery and tissue engineering, where deep tissue penetration and minimal photodamage are critical.[23] This study demonstrates the superior properties of the three-component hydrogel, combining the mechanical and colloidal stability provided by agarose with the tunable dynamics of the photoresponsive LMWG network, now manipulated by NIR irradiation facilitated by UCNP.[24–26]

Results and discussion

To facilitate the isomerization of the AAP peptide, the quantum yield of the UCNP in the UV region was enhanced by optimizing the lanthanide composition in the UCNP (Fig. 2). The UCNP are composed of $LiYF_4$ doped with 0.5 mol% Tm^{3+} and

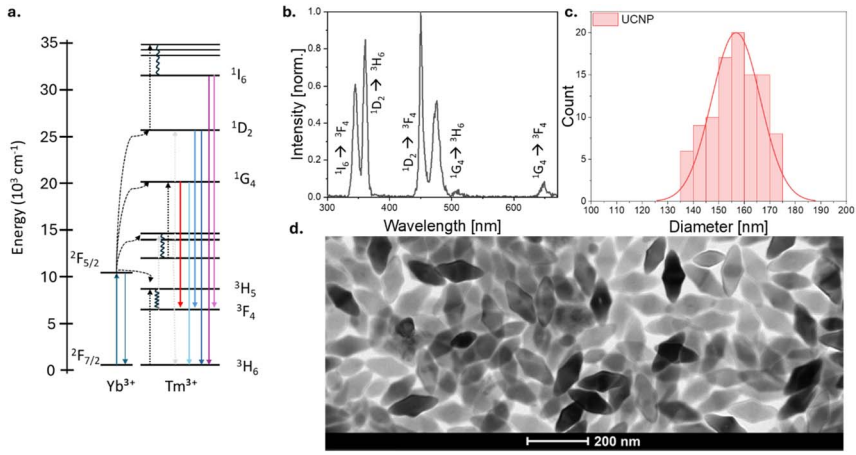

Fig. 2 (a) Energy-level diagram illustrating the upconversion mechanism facilitated by Yb^{3+} and Tm^{3+} ions in the UCNP. The UCNP are composed of $LiYF_4$ doped with 0.5 mol% Tm^{3+} and 25 mol% Yb^{3+}. (b) Emission spectrum of the UCNP, showing efficient generation of UV light upon excitation at 980 nm. (c) Size distribution of the synthesized UCNP, revealing a particle diameter of 135–175 nm. (d) Transmission electron microscopy (TEM) image of diamond-shaped UCNP.[29,30]

25 mol% Yb^{3+}. This optimization enabled efficient generation of UV irradiation directly from the nanoparticles, eliminating the need for an external UV light source. The mechanism of the upconversion process is schematically illustrated in Fig. 2a. The UCNP were synthesized following the procedure described by Capobianco *et al.*[27] In order to ultimately incorporate the nanoparticles into the hydrogel, water-solubility of the particles was essential. The particles were therefore coated with a silica layer in a further synthesis step.[28] The emission spectrum of the UCNP upon excitation with NIR at 980 nm is shown in Fig. 2b, indicating pronounced emission in the UV range around 350 nm. Transmission electron microscopy revealed that the synthesized UCNP exhibit a diamond-like morphology with an average diameter of approximately 150–160 nm. The particle size distribution is provided in Fig. 2c and a transmission electron microscopy image is shown in Fig. 2d. Additional TEM analysis is provided in the ESI Fig. S6.†

The gelator AAP-FGDS shown in Fig. 1 was produced using solid-phase peptide synthesis, following a standard protecting group strategy. The AAP carboxylic acid was used to introduce the photoresponsive moiety at the N-terminus of the peptide FGDS. This gelator was synthesized and described previously by our team.[7] Details of the synthesis and analysis of AAP-FGDS are provided in the ESI.† The preparation of homogeneous hydrogels was achieved through a heating–cooling cycle. AAP-FGDS (3 wt%), agarose (1.5 wt%), and UCNP (0.1 wt%) were dissolved in water. Agarose was introduced to the peptide system to support the gel structure and provide enhanced mechanical and colloidal stability. While the individual gelator AAP-FGDS is capable of forming hydrogels, the resulting gels are not as robust, and significantly higher concentrations of the gelator would be required to achieve similar mechanical properties. The pH of the solution was adjusted to pH = 11 using a KOH solution, and the mixture was sonicated for

10 min to ensure complete dissolution. The solution was subsequently heated in an oven at 90 °C for 5 min before being allowed to cool to room temperature, yielding a uniform hydrogel formulation.

In Fig. 3a, the inverted vial test demonstrates the gel's phase transitions through three distinct states: (1) a self-supporting gel upon preparation, (2) a soft and liquefied state induced by irradiation with a 980 nm NIR laser, and (3) re-formation of the self-supporting gel upon irradiation with green light (520 nm). These transitions are clearly driven by the photoisomerization of the AAP-FGDS peptide, which switches from the *E*-isomer to the *Z*-isomer under NIR irradiation. Even if the photoisomerization is rather slow and incomplete, the degree of conversion is sufficient to disrupt the supramolecular network of the hydrogel and transition the gel into a soft and liquefied state. Negative control experiments showed no changes in the UV band during irradiation (see ESI Fig. S8†).

Fig. 3b provides evidence supporting the observed isomerization process through UV-Vis spectra, which demonstrate a decrease in the $\pi \rightarrow \pi^*$ absorption band at 330 nm. These spectral changes are consistent with the photoisomerization of AAP from the *E*-isomer to the *Z*-isomer. Upon irradiation with 980 nm, the transition from the *E*-isomer to the *Z*-isomer was confirmed within

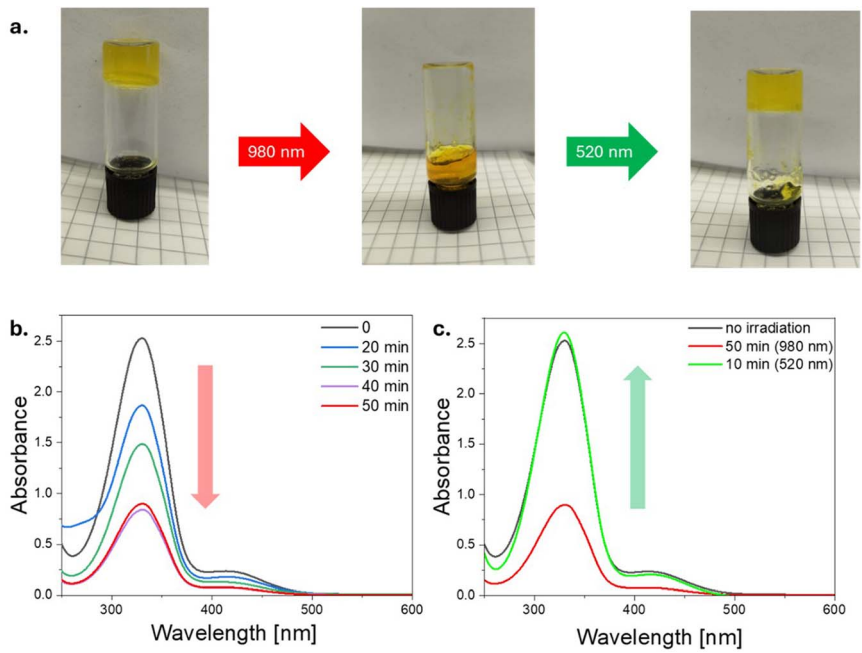

Fig. 3 Light-induced phase transitions and isomerization of the three-component hydrogel. (a) Inverted vial test showing the gel's transition from self-supporting (pre-NIR irradiation), to soft/liquefied (980 nm NIR irradiation), and back to self-supporting states (520 nm visible light). These transitions are driven by the photoisomerization of the AAP-FGDS peptide. (b) UV-Vis spectra confirming the photoisomerization, with a decrease in the $\pi \rightarrow \pi^*$ absorption band and characteristic spectral shifts indicating the transition from the *E*-isomer to the *Z*-isomer under 980 nm irradiation. (c) UV-Vis spectra demonstrating reversible switching back to the *E*-isomer upon exposure to visible light at 520 nm, restoring the initial spectrum and the gel's self-supporting state.

50 min based on characteristic spectral shifts. While the degree of conversion remains limited, it is sufficient to enable switching between gel states, underscoring the material's efficiency and reversibility in response to light stimuli. Subsequent exposure to visible light at 520 nm fully restored the original spectrum, demonstrating the reversible photoisomerization back to the thermodynamically favored *E*-isomer of the peptide.

The structural organization of the hydrogel and the incorporation of the UCNP were further examined using transmission electron microscopy (TEM) and scanning electron microscopy (SEM), as shown in Fig. 4. The TEM image (Fig. 4a) reveals the fiber structure of the hydrogel in the background, with the darker particles corresponding to the UCNP embedded within the hydrogel. This demonstrates the successful integration of the nanoparticles into the hydrogel network. The SEM image (Fig. 4b) provides a clearer visualization of the fibrous structure of the hydrogel, showing a well-defined network that supports the gel's mechanical properties. Additionally, some UCNP are visible on the surface of the hydrogel, confirming their homogeneous distribution. Additional TEM analysis is provided in the ESI Fig. S7.†

Fig. 5 illustrates the emission spectra of UCNP under different conditions, revealing their behavior in distinct gel matrices. In Fig. 5a, it can be seen that the emission spectra of UCNP in water and agarose gel are nearly identical, with overlapping peaks that indicate no significant alteration in the luminescence properties of the nanoparticles embedded in the agarose gel. This suggests that the agarose environment does not influence the emission characteristics of the UCNP.

In contrast, Fig. 5b compares the emission spectra of UCNP in agarose gel with those in the AAP-FGDS gel. A complete quenching of the UV emission band is observed in the presence of AAP-FGDS, which demonstrates efficient energy transfer between the UCNP and the AAP-FGDS in the gel. Energy transfer effectively suppresses the UV emission from the UCNP, indicating the significant

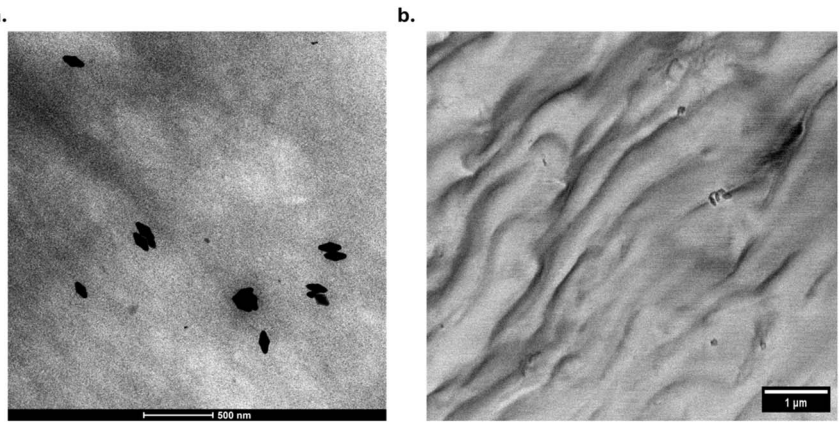

Fig. 4 Microscopy of the three-component hydrogel. (a) TEM image showing the fiber structure of the hydrogel in the background and the darker UCNP embedded within the gel. (b) SEM image providing a clearer visualization of the hydrogel structure, with the fiber arrangement being more distinct and some UCNP visible at the surface of the hydrogel.

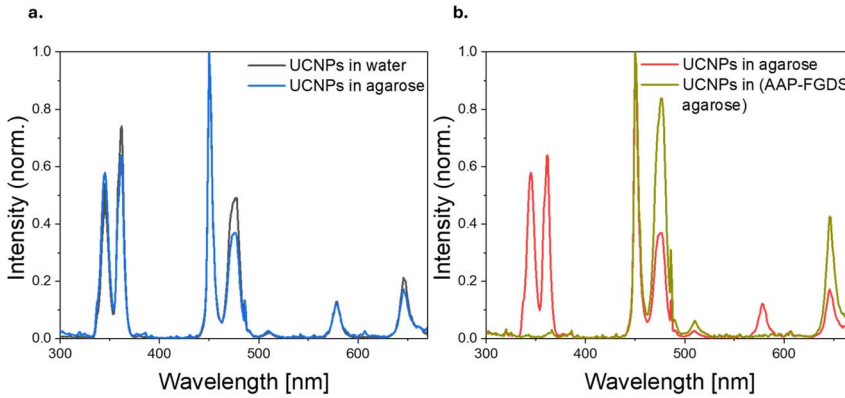

Fig. 5 Emission spectra of UCNP under different conditions. (a) Comparison of UCNP in water and in agarose gel shows no significant change in emission profiles, indicating that agarose does not affect the luminescence properties of the UCNP. (b) Emission spectra of UCNP in agarose gel and in AAP-FGDS gel demonstrate complete quenching of the UV signal in the presence of AAP-FGDS, suggesting efficient energy transfer between the UCNP and the AAP in the gel.

impact of the AAP-FGDS gel on the emission properties of the UCNP and absorbance of the UV emission of the UCNP by the AAP in the three-component gel.

Fig. 6 illustrates the rheological behavior of peptide-based hydrogels before and after exposure to NIR irradiation, highlighting the impact of photoisomerization on the mechanical properties of the gel. Fig. 6a and b focus on the dynamic moduli of the gel as a function of shear strain and frequency. In Fig. 6a, the storage modulus (G') and loss modulus (G'') are plotted against shear strain to assess the elasticity and viscosity of the gel. Before irradiation, the storage modulus (G') dominates the loss modulus (G''), which indicates that the gel structure is predominantly elastic and resists deformation under applied stress. The high G' values relative to G'' signify a cohesive gel network. However, upon irradiation with a 980 nm NIR laser, both G' and G'' decrease significantly, with a pronounced reduction in G'. This shift demonstrates that the gel undergoes considerable softening and a partial loss of its elastic properties is also observed. This behavior can be attributed to photoisomerization within the peptide network, which disrupts the supramolecular interactions that maintain the gel's structural integrity.

Fig. 6b examines the frequency dependence of G' and G'', illustrating how the gel responds to dynamic forces. Both G' and G'' increase with frequency, which is characteristic of viscoelastic materials, reflecting their ability to store and dissipate energy under oscillatory deformation. After NIR irradiation, the moduli remain consistently lower across all frequencies compared to the pre-irradiation state. This reduction indicates that the gel's ability to maintain its structural strength and dissipate energy is impaired by the light-induced disruption of the peptide network. Together, the data confirm that NIR irradiation significantly alters the gel's rheological properties, shifting it from a highly elastic structure to a softer, less cohesive state.

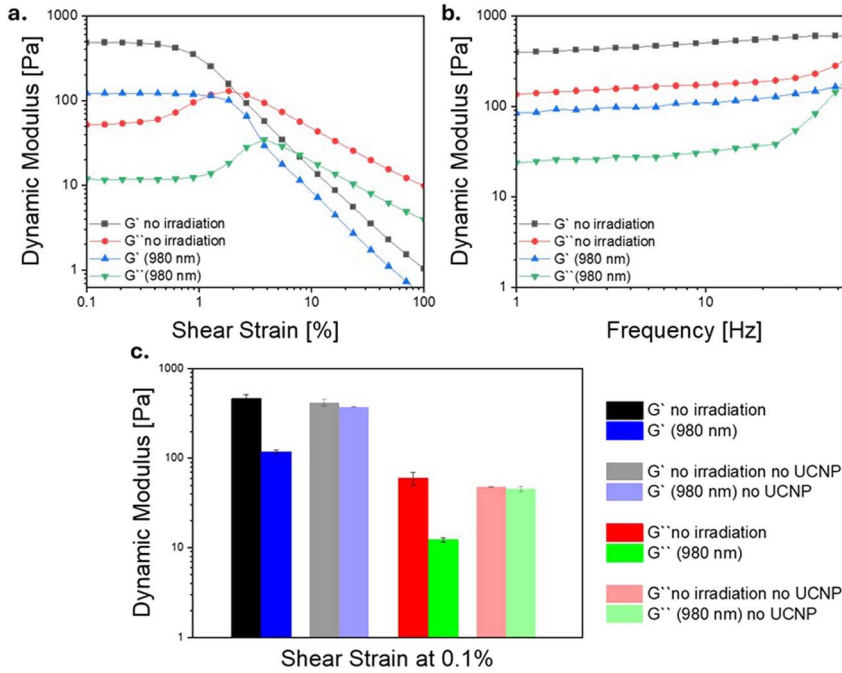

Fig. 6 Rheological analysis of the three-component hydrogels before and after NIR irradiation. (a) Storage modulus (G') and loss modulus (G'') as a function of shear strain, showing a significant decrease in both moduli after irradiation with 980 nm light, with G' exhibiting the largest reduction, indicative of gel softening. (b) Frequency-dependent behavior of G' and G'', where both moduli increase with frequency but remain consistently lower post-irradiation, reflecting a weakened gel structure. (c) Bar chart comparing the storage modulus (G') and loss modulus (G'') of peptide-based hydrogels at 0.1% shear strain before and after irradiation with 980 nm light. A significant reduction in G' highlights the gel's reduced elasticity, while a decrease in G'' demonstrates a corresponding reduction in viscous dissipation. Additionally, negative control measurements conducted without UCNP in the gel, are included to show the consistency of the gel properties under 980 nm irradiation. In the negative experiment, no significant changes in G' or G'' were observed, confirming that the effect of 980 nm irradiation is specific to the presence of UCNP ($n = 3$). Note the logarithmic y-scale in all panels.

Fig. 6c provides a summarized comparison of the gel's mechanical properties before and after irradiation in the form of bar charts. The storage modulus (G') at 0.1% shear strain is clearly reduced after NIR exposure, further emphasizing the weakening of the gel's elasticity. Similarly, a corresponding decrease in the loss modulus (G'') is observed, which reflects a reduction in the gel's viscous dissipation capacity. These experiments were conducted in triplicate, as evidenced by the error bars, which represent the standard deviation of the measurements. Additionally, negative control measurements conducted without UCNP in the gel were performed to test the consistency of the gel properties under 980 nm irradiation. In the negative experiment, no significant changes in G' or G'' were observed (see ESI Fig. S9†), confirming that the effect of 980 nm irradiation is specific to the presence of UCNP, and cannot be due to a thermal effect. Interestingly, also the moduli of gels prepared with and without UCNP

are very similar, indicating that the UCNP do not affect to the mechanical stability of the gel.

In summary, the combined data from all experiments demonstrate that NIR irradiation induces a substantial weakening of the gel's mechanical properties by triggering photoisomerization within the AAP peptide in the three-component hydrogel. This leads to the disruption of the supramolecular interactions that maintain the gel's elasticity and structural integrity, resulting in a softer and less stable material. These findings underline the photoresponsive nature of the hydrogel and its ability to undergo reversible changes of its mechanical properties in response to external stimuli.

Conclusion

This study demonstrates the successful development of a photoresponsive three-component supramolecular hydrogel that combines the mechanical robustness of an agarose network with the dynamic, photoresponsive behavior of a self-assembling peptide-based gelator AAP-FGDS. By incorporating UCNP, the three-component gel achieves precise control over the gel's properties using biocompatible NIR light, eliminating the need for potentially harmful UV irradiation. The reversible gel-to-sol transitions, driven by the isomerization of the AAP-FGDS peptide, enable the material to respond dynamically to external light stimuli, as confirmed by UV-Vis spectroscopy, emission studies and rheological analysis.

The findings highlight the remarkable versatility of the three-component gel. Rheological data reveals significant softening of the gel upon NIR exposure, with its elastic and viscous properties restored upon visible light irradiation. The energy transfer between UCNP and the gel is demonstrated to be essential for efficient NIR-triggered photoisomerization, ensuring reproducibility and stability of the photoresponse. Furthermore, the hybrid gel's tunable mechanical properties and biocompatibility make it a promising candidate for *in vivo* applications, including targeted drug delivery, tissue engineering, and other biomedical uses where deep tissue penetration and minimal photodamage are critical. Thus, this work paves the way for the development of next-generation soft materials with enhanced response and adaptability, providing a platform for the design of multifunctional hydrogels tailored for specific biomedical and nanotechnological applications.

Data availability

The data supporting this article have been included as part of the supplementary information.†

Conflicts of interest

There are no conflicts to declare.

Acknowledgements

This work was funded by the Deutsche Forschungsgemeinschaft (DFG CRC 1459 Intelligent Matter Project ID 433682494).

References

1 R. V. Ulijn and A. M. Smith, Designing peptide based nanomaterials, *Chem. Soc. Rev.*, 2008, **37**, 664–675.
2 R. J. Mart, R. D. Osborne, M. M. Stevens and R. V. Ulijn, Peptide-based stimuli-responsive biomaterials, *Soft Matter*, 2006, **2**, 822–835.
3 M. George and R. G. Weiss, Molecular organogels. Soft matter comprised of low-molecular-mass organic gelators and organic liquids, *Acc. Chem. Res.*, 2006, **39**, 489–497.
4 C. Yuan, Q. Li, R. Xing, J. Li and X. Yan, Peptide self-assembly through liquid-liquid phase separation, *Chem*, 2023, **9**, 2425–2445.
5 S. Panja and D. J. Adams, Stimuli responsive dynamic transformations in supramolecular gels, *Chem. Soc. Rev.*, 2021, **50**, 5165–5200.
6 R. Chang, C. Yuan, P. Zhou, R. Xing and X. Yan, Peptide Self-assembly: From Ordered to Disordered, *Acc. Chem. Res.*, 2024, **57**, 289–301.
7 B. P. Nowak and B. J. Ravoo, Photoresponsive hybrid hydrogel with a dual network of agarose and a self-assembling peptide, *Soft Matter*, 2020, **16**, 7299–7304.
8 B. Yan, J.-C. Boyer, D. Habault, N. R. Branda and Y. Zhao, Near Infrared Light Triggered Release of Biomacromolecules from Hydrogels Loaded with Upconversion Nanoparticles, *J. Am. Chem. Soc.*, 2012, **134**, 16558–16561.
9 J. Tang, J. Ou, C. Zhu, C. Yao and D. Yang, Flash Synthesis of DNA Hydrogel via Supramacromolecular Assembly of DNA Chains and Upconversion Nanoparticles for Cell Engineering, *Adv. Funct. Mater.*, 2022, **32**, 2107267.
10 W. Wu, L. Wang, J. Yuan, Z. Zhang, X. Zhang, S. Dong and J. Hao, Formation and Degradation Tracking of a Composite Hydrogel Based on UCNPs@PDA, *Macromolecules*, 2020, **53**, 2430–2440.
11 J. Liu, B. Zhang, Z. Lu, J. Shen, P. Zhang and Y. Yu, Interfacial Engineering of High-Performance Upconversion Hydrogels with Orthogonal NIR Photochemistry in vivo for Synergistic Noninvasive Biofilm Elimination and Tissue Repair, *Chem. Mater.*, 2024, **36**, 6276–6287.
12 B. P. Nowak and B. J. Ravoo, Magneto- and photo-responsive hydrogels from the co-assembly of peptides, cyclodextrins, and superparamagnetic nanoparticles, *Faraday Discuss.*, 2019, **219**, 220–228.
13 B. P. Nowak, M. Niehues and B. J. Ravoo, Magneto-responsive hydrogels by self-assembly of low molecular weight peptides and crosslinking with iron oxide nanoparticles, *Soft Matter*, 2021, **17**, 2857–2864.
14 N. Möller, T. Hellwig, L. Stricker, S. Engel, C. Fallnich and B. J. Ravoo, Near-infrared photoswitching of cyclodextrin–guest complexes using lanthanide-doped $LiYF_4$ upconversion nanoparticles, *Chem. Commun.*, 2017, **53**, 240–243.
15 X. An, L. Gao, J. Guo, F. Meng, H. Lian, S. Zhang, J. L. Pathak, Y. Li and S. Zhang, Rare-earth doped upconversion-photopolymerization hydrogel hybrids for *in vivo* wound healing, *J. Mater. Chem. C*, 2025, **13**, 1999–2009, DOI: **10.1039/D4TC04309J**.
16 T. R. Hoare and D. S. Kohane, Hydrogels in drug delivery: Progress and challenges, *Polymer*, 2008, **49**, 1993–2007.
17 X. Hu, D. Zhang and S. S. Sheiko, Cooling-Triggered Shapeshifting Hydrogels with Multi-Shape Memory Performance, *Adv. Mater.*, 2018, **30**, e1707461.

18 A. M. Brizard, M. C. A. Stuart and J. H. van Esch, Self-assembled interpenetrating networks by orthogonal self assembly of surfactants and hydrogelators, *Faraday Discuss.*, 2009, **143**, 345–357.
19 P. R. A. Chivers and D. K. Smith, Spatially-resolved soft materials for controlled release – hybrid hydrogels combining a robust photo-activated polymer gelwith an interactive supramolecular gel, *Chem. Sci.*, 2017, **8**, 7218–7227.
20 C.-W. Chu and B. J. Ravoo, Hierarchical supramolecular hydrogels: self-assembly by peptides and photo-controlled release *via* host–guest interaction, *Chem. Commun.*, 2017, **53**, 12450–12453.
21 D. J. Abdallah and R. G. Weiss, Organogels and Low Molecular Mass Organic Gelators, *Adv. Mater.*, 2000, **12**, 1237–1247.
22 D. J. Cornwell, B. O. Okesola and D. K. Smith, Hybrid polymer and low molecular weight gels – dynamic two-component soft materials with both responsive and robust nanoscale networks, *Soft Matter*, 2013, **9**, 8730.
23 D. J. Cornwell and D. K. Smith, Expanding the scope of gels – combining polymers with low-molecular-weight gelators to yield modified self-assembling smart materials with high-tech applications, *Mater. Horiz.*, 2015, **2**, 279–293.
24 M. de Loos, B. L. Feringa and J. H. van Esch, Design and Application of Self-Assembled Low Molecular Weight Hydrogels, *Eur. J. Org. Chem.*, 2005, **2005**, 3615–3631.
25 D. J. Adams, M. F. Butler, W. J. Frith, M. Kirkland, L. Mullen and P. Sanderson, A new method for maintaining homogeneity during liquid–hydrogel transitions using low molecular weight hydrogelators, *Soft Matter*, 2009, **5**, 1856.
26 L. E. Buerkle and S. J. Rowan, Supramolecular gels formed from multi-component low molecular weight species, *Chem. Soc. Rev.*, 2012, **41**, 6089–6102.
27 V. Mahalingam, F. Vetrone, R. Naccache, A. Speghini and J. A. Capobianco, Colloidal Tm^{3+}/Yb^{3+}-Doped $LiYF_4$ Nanocrystals: Multiple Luminescence Spanning the UV to NIR Regions via Low-Energy Excitation, *Adv. Mater.*, 2009, **21**, 4025–4028.
28 H. L. Ding, Y. X. Zhang, S. Wang, J. M. Xu, S. C. Xu and G. H. Li, Fe_3O_4@SiO_2 Core/Shell Nanoparticles: The Silica Coating Regulations with a Single Core for Different Core Sizes and Shell Thicknesses, *Chem. Mater.*, 2012, **24**, 4572–4580.
29 *Handbook on the Physics and Chemistry of Rare Earths*, ed. J.-C. Bünzli and V. K. Pecharsky, Elsevier, 2015.
30 S. L. Maurizio, G. Tessitore, G. A. Mandl and J. A. Capobianco, Luminescence dynamics and enhancement of the UV and visible emissions of Tm^{3+} in $LiYF_4$:Yb^{3+},Tm^{3+} upconverting nanoparticles, *Nanoscale Adv.*, 2019, **1**, 4492–4500.